

# Experimental Study on Heat Transfer Characteristics of Dynamic Leidenfrost Droplets

Hyunwoong Lee <sup>a</sup>, Hyungdae Kim <sup>a\*</sup>

<sup>a</sup>Department of Nuclear Engineering, Kyung Hee University, Republic of Korea

\*Corresponding author: hdkims@khu.ac.kr

## 1. Introduction

Droplet-wall direct contact heat transfer in dispersed flow film boiling is one of the key heat transfer mechanisms while overheated nuclear fuels by loss of coolant accident (LBLOCA) are reflooded by the injected coolant by the emergency core cooling system. Dynamic Leidenfrost point temperature (DLPT) is defined as the minimum temperature when the impinging droplet is rebounded up from the heated solid surface, by forming a stable vapor film layer. Most previous experiments determined DLPT only based on dynamics of impinging droplets on hot surfaces while neglecting variation of actual heat transfer amount during collisions. In fact, it is hard to accurately measure the heat transfer characteristics associated with transient dynamic collision of droplets on hot surface.

Seiler-Marie et al. [1] recently reported an interesting finding about the so-called ‘shoulder of flux’ phenomenon in experiments of impinging jets on very hot plates: a secondary maximum heat flux point was observed in transition boiling regime at much higher temperatures than the critical heat flux point temperature. This may indicate heat transfer behaviors associated with dynamic Leidenfrost droplets might not as simple as we believe.

The objective of this study is to experimentally investigate heat transfer characteristics of dynamic Leidenfrost droplets by varying heated surface temperature in the wide range from 200°C to 600°C. To accurately measure the amount of heat transfer during collision of single droplets onto hot surface, temporal temperature distribution of the collision wall was measured using high-speed infrared camera and associated heat transfer rate was calculated by solving transient heat conduction in the heated wall during the collision.

## 2. Experiment

### 2.1. Experimental setup and procedure

Fig. 1 shows the schematic of the experimental apparatus for single droplet experiment. Droplets are produced through 31-gauge needle ( $D_o = 260 \mu\text{m}$ ,  $D_i = 130 \mu\text{m}$ , Hamilton Inc.) connected to water tanks. Droplet temperature is controlled by a band heater attached to the water tank and single droplets are generated using a loaded syringe pump (KSD-100, KD Scientific Inc.). Droplets are impinged onto the sample by gravity. Droplet speed is adjusted by the height of the clamp by which the needle is fixed.

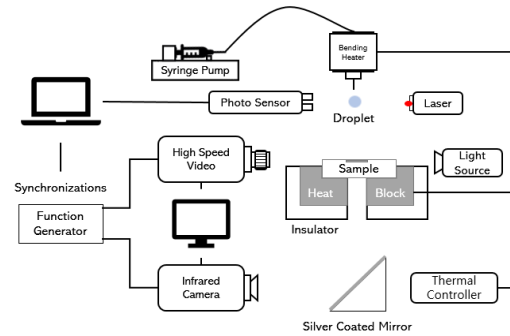


Figure 1. Schematic of experimental apparatus

Table I: Specifications of IR and HSV

	IR	HSV
Frame rates (kHz)	2	10
Window size (pixels)	54 × 54	290 × 290
Spatial resolution (μm)	145	27

The sample in which droplets impinged consists of a circular sapphire with a diameter of 25 mm and a thickness of 5 mm. A thin platinum film which is 20 mm diameter and 100 nm thick is deposited. The sample is placed on a SS304 heating block with four 200-W embedded cartridge heaters. The heating block underneath the sapphire sample has a hole of 20mm diameter at the center from bottom. Through the hole, two-dimensional distribution of thermal radiation from the platinum film can be measured using a high-speed infrared (IR) camera (FLIR SC-6000).

Dynamic characteristics of droplets during collision are observed using a high-speed video camera (Phantom V7.3, Vision Research Inc.) from side. The HSV camera and IR camera are controlled by the function generator with synchronization, at which point the trigger is determined by the signal from the photo sensor that causes the liquid fall. The specifications used by IR cameras and HSV cameras in this experiment are summarized in Table 1.

### 2.2. Experimental conditions

The independent variables of the experiment are set to be We number and collision wall temperature. Droplet temperature is set at 90°C which is close to saturation temperature and its diameter size is fixed at 2mm. We number is set 110. Then, the wall temperature varies up to 700°C

### 2.3. Data analysis

#### 2.3.1. Surface heat flux calculation

The high speed IR camera permits to measure history of temperature distribution at the top surface of the sample during droplet collision. The temperature data is used as the boundary condition for three-dimensional transient conduction analysis inside the sapphire sample, along with appropriate boundary conditions for the side and bottom surfaces as shown in Fig. 2.

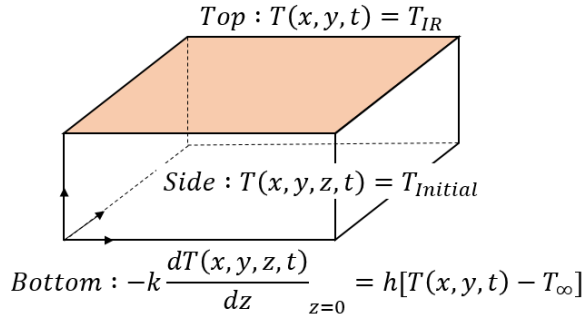


Figure 2. Boundary conditions and model geometry

The three-dimensional conduction analysis is conducted using ANSYS Fluent. Finally, the heat flux distribution at the collision surface from the wall to droplet is calculated from the obtained temperature data as follow.

$$q''_{top} = -k \left. \frac{\partial T}{\partial z} \right|_{z=0} \quad (1)$$

#### 2.3.2. Total heat transfer by droplet collision

The total heat transfer amount by single droplet collision is calculated by integrating the wall heat flux distribution for its residence time as follow.

$$Q = \int_0^{t_k} \int_A q''_{top}(x, y, t) dA \quad (2)$$

The residence time and heat transfer area of the integral are determined using the method previously introduced in [3, 4].

## 3. Results and Data Interpretation

### 3.1. Thermal characteristics and droplet dynamics

Figure 3 shows the visualization results of the collision dynamics, temperature and heat flux changes after the impact of the droplet at 300°C.

A comparison of Figs. 4 and 5 shows a rapid increase in heat flux at 300 °C, a rise in temperature again, and a distinct reduction in heat flux value between 300°C and 500°C.

Table II: Thermo-physical properties of sapphire (400°C)

Properties	Values
$\rho(\text{kg}/\text{m}^3)$	3917
$C_p(\text{J}/\text{kg} \cdot \text{K})$	945
$k(\text{W}/\text{m} \cdot \text{K})$	27
$\alpha(\text{m}^2/\text{s})$	$2.79 \times 10^{-5}$

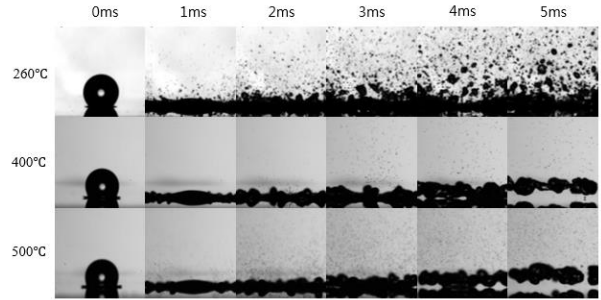


Figure 3. Disintegration of droplet according to wall temperature change @  $We = 110$

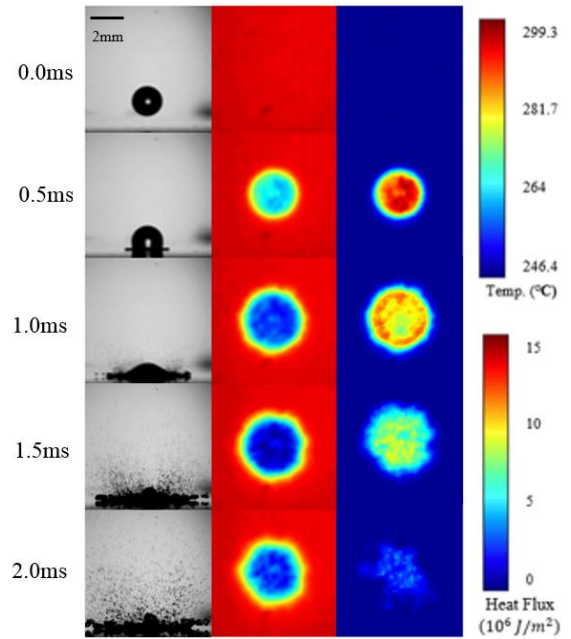


Figure 4. Dynamics, temperature and heat flux of droplet after collisions @  $We = 110$

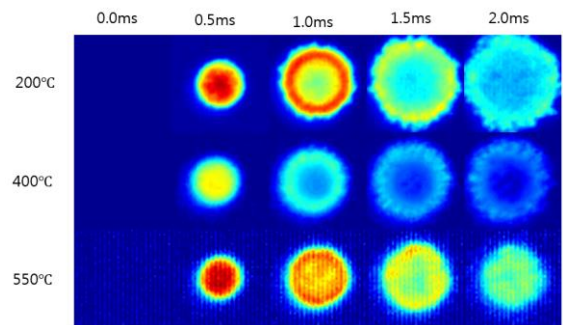


Figure 5. Heat flux according to time and wall temperature @  $We = 110$

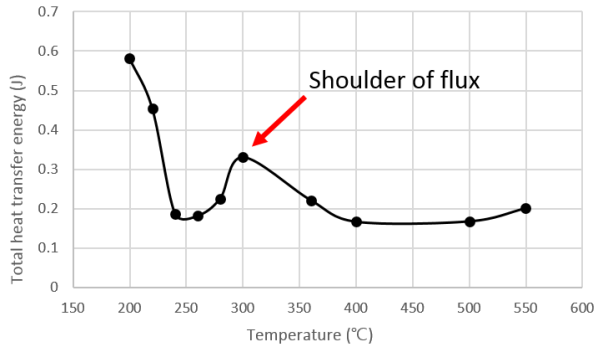


Figure 6. Total energy removal by droplet,  $We = 110$

### 3.2. Heat transfer rate vs. wall temperature

Figure 6 shows a variation of total energy removal by droplet at  $We = 110$  as a function of wall temperature. In most previous studies, linearly decreasing tendency of heat transfer was observed near LPT as increasing wall temperature. However, the shoulder of flux phenomenon previously reported by Seiler-Marile et al. [2] appeared in the present study. As seen in Fig. 6, a secondary peak of heat transfer amount was observed at a temperature higher than LFP. Such behavior is not observed in stationary Leidenfrost droplets. In this regard, it is supposed that the observed shoulder of flux behavior might be associated with dynamics of droplets impacting onto the hot wall. To completely understand the causes of the shoulder of flux phenomenon, further systemic studies as varying droplet velocity are needed.

## 4. Conclusions

Heat transfer characteristics associated with dynamic droplets ( $We = 110$ ) colliding onto a hot surface above so-called Leidenfrost temperature were experimentally studied. The interesting variation of heat transfer amount was observed as increasing wall temperature in the range above Leidenfrost temperature: a secondary heat flux peak, so-called shoulder of flux, appeared. This change in heat transfer characteristics associated with dynamic droplets might make an impact on fuel cladding cooling via droplet dispersed flow film boiling in the reflow phase of LOCA analysis. In the reflowing phase of LOCA analysis, which used to be interpreted only as film boiling, heat transfer specific phenomena above Leidenfrost temperature will add a method of heat transfer analysis of two phase flow, which will serve as the basis for more precise identification of the situation after a severe accident. Therefore, follow-up studies should be conducted to clearly understand why this phenomenon happens.

## ACKNOWLEDGMENTS

This work was supported by a grant from the National Research Foundation of Korea (NRF No.2019M2D2A1 A0205936412) funded by the Korea government (MSIT)

## REFERENCES

- [1] K.J.Choi, S.C.Yao, Mechanisms of film boiling heat transfer of normally impacting spray, *International Journal of Heat and Mass Transfer*, vol.30, 1987
- [2] N.Seiler-Marie, J.Seiler, O.Simonin, Transition boiling at jet impingement, *International Journal of Heat and Mass Transfer*, vol.47, 2004
- [3] R.Cgen, S.Chiu, Resident time of a compound drop impinging on a hot surface, *Applied Thermal Engineering*, vol.27, 2007
- [4] J.Jung, S.Jeong, H.Kim, Investigation of single-droplet/wall collision heat transfer characteristics using infrared thermometry, *International Journal of Heat and Mass Transfer*, vol.92, 2016.